Environmental Science and Pollution Research (2022) 29:91212–91231
https://doi.org/10.1007/s11356-022-22036-6

RESEARCH ARTICLE

Thermal bioclimatic indicators over Southeast Asia: present status and future projection using CMIP6

Mohammed Magdy Hamed[1,2] · Mohamed Salem Nashwan[3] · Shamsuddin Shahid[2] · Tarmizi bin Ismail[2] · Ashraf Dewan[4] · Md Asaduzzaman[5]

Received: 22 December 2021 / Accepted: 11 July 2022 / Published online: 26 July 2022

Abstract

Mapping potential changes in bioclimatic characteristics are critical for planning mitigation goals and climate change adaptation. Assessment of such changes is particularly important for Southeast Asia (SEA) — home to global largest ecological diversity. Twenty-three global climate models (GCMs) of Coupled Model Intercomparison Project Phase 6 (CMIP6) were used in this study to evaluate changes in 11 thermal bioclimatic indicators over SEA for two shared socioeconomic pathways (SSPs), 2–4.5 and 5–8.5. Spatial changes in the ensemble mean, 5th, and 95th percentile of each indicator for near (2020–2059) and far (2060–2099) periods were examined in order to understand temporal changes and associated uncertainty. The results indicated large spatial heterogeneity and temporal variability in projected changes of bioclimatic indicators. A higher change was projected for mainland SEA in the far future and less in maritime region during the near future. At the same time, uncertainty in the projected bioclimatic indices was higher for mainland than maritime SEA. Analysis of mean multi-model ensemble revealed a change in mean temperature ranged from − 0.71 to 3.23 °C in near and from 0.00 to 4.07 °C in far futures. The diurnal temperature range was projected to reduce over most of SEA (ranging from − 1.1 to − 2.0 °C), while isothermality is likely to decrease from − 1.1 to − 4.6%. A decrease in isothermality along with narrowing of seasonality indicated a possible shift in climate, particularly in the north of mainland SEA. Maximum temperature in the warmest month/quarter was projected to increase a little more than the coldest month/quarter and the mean temperature in the driest month to increase more than the wettest month. This would cause an increase in the annual temperature range in the future.

Keywords Global climate model · Southeast Asia · Shared socioeconomic pathways · Climate change · Uncertainty

Responsible Editor: Philippe Garrigues

✉ Mohammed Magdy Hamed
eng.mohammedhamed@aast.edu

Mohamed Salem Nashwan
m.salem@aast.edu

Shamsuddin Shahid
sshahid@utm.my

Tarmizi bin Ismail
tarmiziismail@utm.my

Ashraf Dewan
A.Dewan@curtin.edu.au

Md Asaduzzaman
Md.Asaduzzaman@staffs.ac.uk

[1] Construction and Building Engineering Department, College of Engineering and Technology, Arab Academy for Science, Technology and Maritime Transport (AASTMT), B 2401 Smart Village, Giza 12577, Egypt

[2] Department of Water and Environmental Engineering, School of Civil Engineering, Faculty of Engineering, Universiti Teknologi Malaysia (UTM), 81310 Skudia, Johor, Malaysia

[3] Construction and Building Engineering Department, College of Engineering and Technology, Arab Academy for Science, Technology and Maritime Transport (AASTMT), Elhorria, Cairo 2033, Egypt

[4] Spatial Sciences Discipline, School of Earth and Planetary Sciences, Curtin University, Kent Street, Bentley, Perth 6102, Australia

[5] Department of Engineering, School of Digital, Technologies and Arts, Staffordshire University, Stoke-on-Trent, UK

Introduction

Annual and seasonal bioclimate information is essential to understanding climate influences on different species (O'Donnell and Ignizio, 2012). The information is also critical for estimating wildlife distribution (Molloy et al. 2014; Yoon and Lee 2021), farming potential (Kriticos et al. 2012), human comfort (Çaliskan et al. 2013), and vulnerability to climate change (Theusme et al. 2021). Global warming has altered the climate in different ways in different regions of the world (Asadollah et al. 2021; Song et al. 2021; Salehie et al. 2022c). Climate change has changed several climatic characteristics intricately connected to the biosphere (Pour et al. 2019). Minor climate change may significantly affect biological distribution (Hu et al. 2015; Sintayehu 2018), such as a shift in species distribution as the plants and animals would change their locations for survival (Bellard et al., 2012; Molloy et al., 2014; Waltari et al., 2014). The phenology and physiology of many plants may also change in response to climate variability (Bellard et al. 2012). It could also alter people's comfort and elevate public health risks in different regions (Ragheb et al. 2016; Duanmu et al. 2017).

Bioclimatic indicators are increasingly used to analyze the effects of climate change on bio-environment (Rehfeldt et al. 2015; Daham et al. 2018; Ribeiro et al. 2019). Mapping potential changes in bioclimatic characteristics are critical for achieving climate change adaptation and mitigation goals. Future projection of bioclimatic indicators is particularly important for Southeast Asia (SEA) because it is one of the most climate-vulnerable regions of the world resulting from significant ocean-land–atmosphere interactions (Raitzer et al. 2015; Vinke et al. 2017). It is in the center of the Asian monsoon system and at the crossroad of the Asian monsoon's interactions with El Niño–Southern Oscillation (ENSO), the Pacific and Indian Oceans and Northern and Southern Hemispheres. Four SEA nations are among the top ten most vulnerable countries to climate change in the world (Eckstein et al. 2017). According to a recent study (Raitzer et al. 2015), the SEA region's gross domestic product would decline by 11% by the end of this century as a result of climate change, the highest on the planet. Agriculture and ecological industries would be the two most affected areas. Crop yields could drop significantly, and biome shifts might negatively affect ecosystems and livelihood of millions (Woetzel et al. 2020).

The complicated land–ocean boundary and highly irregular geographic variability have made the climate simulation in SEA challenging, particularly using coarse resolution global climate models (GCMs) (Robertson et al. 2011). However, GCMs of different CMIPs have been extensively used for climate simulations and climate change impact assessments in SEA over the past three decades (Moron et al. 1998; Lau and Nath 2000; Abe et al. 2003; Mochizuki et al. 2007; Schiemann et al. 2014; Iqbal et al. 2021; Khadka et al. 2021; Supharatid et al. 2022). Several studies assessed the effect of climate change on the distribution of plants (van Zonneveld et al. 2009; Redfern et al. 2012), animals, and fishing industry in SEA (Abdullah 2003; Asif 2019; Yoon and Lee 2021). Redfern et al. (2012) studied the impact of temperature rise, drought, salinity, rising sea levels, submergence, and socioeconomic factors on rice production in SEA countries. Asif (2019) studied environmental impact on marine resources, such as the fishing industry on Cambodia's coast associated human migration. Yoon and Lee (2021) used bioclimatic indicators to study the distribution of two different pests.

Researchers used raw and downscaled GCMs to assess climate change impacts on biodiversity (Banerjee et al. 2019; Dai et al. 2021; Wang et al. 2021). Banerjee et al. (2019) used the niche overlap method between species to predict the potential distribution under climate change scenarios using Coupled Model Intercomparison Project Phase 5 (CMIP5). Dai et al. (2021) studied the distribution of two different bears associated with climate warming using CMIP5 at current and far future (2070) in China. Wang et al. (2021) examined the projected future distribution of six species of flowering plants at present and future using CMIP5. Thus, assessing bioclimatic indicators in historical and future scenarios across SEA is crucial for sustainable development of the region.

SEA experienced an overall increase of 0.1 °C/decade in mean temperature in the past 50 years (IPCC 2007). Climate extremes in the region also showed a significant variability during this period (Nasional BPP 2012). The temperature is projected to increase by 1.99 and 4.29 °C at the end of the century for Shared Socioeconomic Pathways (SSPs) 2–4.5 and 5–8.5, respectively (Supharatid and Nafung 2021; Hamed et al. 2022a). The extremes are expected to be more frequent in the future due to the rise in temperature, placing SEA at danger of climate change repercussions (Nashwan et al. 2018; Ge et al. 2019).

The purpose of this work is to quantify historical bioclimatic indicators and their future change in SEA under medium and high climate change scenarios. These indicators with biological significance could help researchers better understand species' reactions to climate change (Pour et al. 2019). This is the first attempt to project bioclimate of SEA using recently released CMIP6 models. The novelty of this study is the use of readily available climate projection data to assess possible changes in bio-environment in the two future

periods and two climate change scenarios. Additionally, it may be used to assist policymakers in developing appropriate mitigation and adaptation strategies to climate change in the SEA.

Materials and methods

Study area

SEA consists of 11 countries, having a total population of 563 million with a land area of 4.3 million km^2 (Fig. 1). There are seas, land, and many islands in the region; however, it consists of two primary regions (i.e., Mainland and Maritime SEA). Most of SEA's topography is flat, except for Myanmar and Indonesia, where altitudes can be as high as 4000 m. It is one of the world's most vulnerable regions to climate change because of its unique geographic and meteorological conditions together with socioeconomic and demographic features (Raitzer et al. 2015; Vinke et al. 2017). SEA has a mean annual temperature of 25.0 °C, and a mean annual rainfall is between 700 and 5000 mm, while the mean maximum and minimum temperatures were 30.82 and 20.27 °C, respectively (Peel et al. 2007; Yang et al. 2021). Natural atmospheric processes that cause climate-related catastrophes such as droughts, floods, and other weather events have different spatial and temporal variations (Nashwan et al. 2018; Kuo et al. 2020).

Global climate models

Twenty-three CMIP6 models' monthly rainfall T_{max} and T_{min} simulations for the historical and future projections are used. The GCMs (Table 1) are chosen based on the availability of projected rainfall, maximum (T_{max}) and minimum (T_{min}) monthly temperature for historical, and two SSPs, 2–4.5 and 5–8.5. Outputs of the models are acquired via https://esgf-node.llnl.gov/search/cmip6/. Historical experiment covers 1975–2014, while future experiments (i.e., SSP2-4.5 and SSP5-8.5) cover 2020–2099. The SSP2-4.5 implies middle of the scenarios, taking the rise of mean global temperature to 2.7 °C by 2100. Contrarily, SSP5-8.5 represents the worst-case scenario in CMIP6 with double CO_2 emissions by 2050 compared to its current level and warming of 4.4 °C by the end of this century. Thus, employing these two future scenarios can reflect variability in climate parameters for two possible pathways under climate warming.

Methodology

This study examines the change in biothermal indicators in SEA for different future scenarios. Table 2

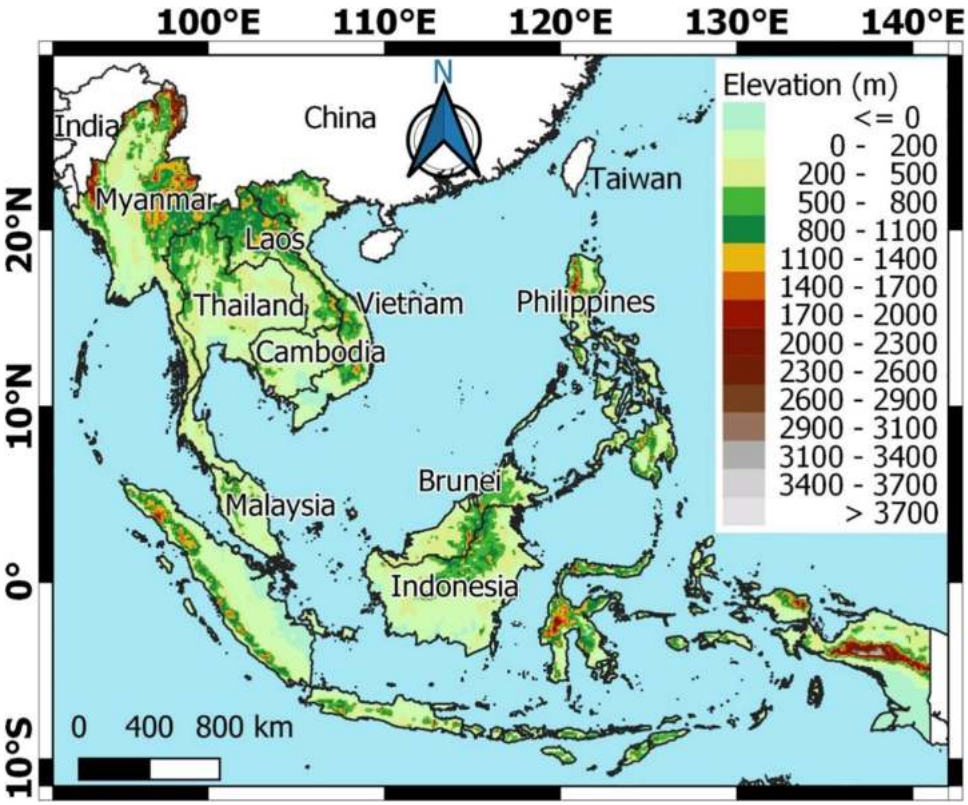

Fig. 1 The location and topography of Southeast Asia

Table 1 CMIP6 GCMs used in the study

No	Model	Institution	Country	Raw nominal resolution (km)	Reference
1	ACCESS-CM2	CSIRO-ARCCSS	Australia	250	(Dix et al. 2019)
2	ACCESS-ESM1-5			250	(Ziehn et al. 2019)
3	AWI-CM-1–1-MR	AWI	Germany	100	(Semmler et al. 2018)
4	BCC-CSM2-MR	BCC	China	100	(Wu et al. 2018)
5	CanESM5	CCCMA	Canada	500	(Swart et al. 2019)
6	CAS-ESM2-0	CAS-ESM	China	100	(Chai 2020)
7	CIESM	CIESM	China	100	(Huang 2019)
8	CMCC-ESM2	CMCC	Italy	100	(Peano et al. 2020)
9	EC-Earth3	EC-Earth	Europe	100	(Döscher et al. 2021)
10	EC-Earth3-CC			100	
11	EC-Earth3-Veg			100	
12	EC-Earth3-Veg-LR			100	
13	FGOALS-g3	FGOALS	China	250	(Pu et al. 2020)
14	FIO-ESM-2–0	FIO	China	100	(Song et al. 2019)
15	GFDL-ESM4	NOAA-GFDL	USA	100	(Krasting et al. 2018)
16	INM-CM4-8	INM	Russia	100	(Volodin et al. 2019a)
17	INM-CM5-0			100	(Volodin et al. 2019b)
18	IPSL-CM6A-LR	IPSL	France	250	(Boucher et al. 2018)
19	MIROC6	MIROC	Japan	250	(Tatebe et al. 2019)
20	MPI-ESM1-2-HR	MPI-M	Germany	100	(von Storch et al. 2017)
21	MPI-ESM1-2-LR			250	(Wieners et al. 2019)
22	MRI-ESM2-0	MRI	Japan	100	(Yukimoto et al. 2019)
23	NESM3	Nanjing University	China	250	(Cao and Wang 2019)

provides comprehensive explanations of the indicators used (O'Donnell and Ignizio 2012). Among the 11 indicators, five are annual indicators (Bio-1, Bio-2, Bio-3, Bio-4, and Bio-7), four are seasonal indicators (Bio-5, Bio-6, Bio-10, and Bio-11) and two are limiting environment indicators (Bio-8 and Bio-9). This methodological flow starts with interpolating raw GCM models' outputs into a common 1.0° spatial resolution, nearly to the mean resolution of all GCMs, via bilinear interpolation discussed in Hamed et al. (2021). This guarantees that the results are not biased due to different spatial representations of raw GCMs (see Table 1) (Nashwan and Shahid 2020). The raw GCMs preserve the original climate change signal (Salehie et al. 2022a, b). Then, different indicators were computed for each model output for the historical period and two future scenarios. For Bio-8 to Bio-11, a dynamic method was followed to select the maximum or minimum temperature month. The selected maximum and minimum temperature/rainfall months for the historical and future periods were not fixed. They were reselected for the future periods (Bede-Fazekas and Somodi 2020). A historical mean multi-model ensemble (MME) was created using 23 GCMs' outputs to decrease uncertainty and represent the 5th and 95th percentile or confidence interval (CI) in the change of each indicator. The MME mean and percentiles were also computed for the two projected periods (e.g., near 2020–2059 and far 2060–2100) for SSP2-4.5 and SSP5-8.5. The historical MME estimations were subtracted from the MME projections for the future periods to calculate the changes in the future periods.

Results

Thermal bioclimatic indicators, estimated using different GCMs, are used to form an MME. The following sections present the historical MME mean of each indicator employed in this study. Besides, projected changes in MME mean and 5th and 95th percentiles for each indicator for near and far futures, under SSP2-4.5 and SSP5-8.5, are presented. The 5th and 95th percentiles are presented to show the 90-percentile confidence interval (CI) or the uncertainty in the changes.

Annual indicators

Annual mean temperature and diurnal temperature range

Spatial distribution of annual mean temperature (Bio-1) at different grids over SEA is presented in Fig. 2, while diurnal

Table 2 Definition of the bioclimatic indicators where T_{avg} is the mean temperature (($T_{max}+T_{min}$)/2), and i is the month of the year

Indicator	Equation	Unit
Annual indicators		
Bio-1 annual mean temperature	$Bio1 = \frac{\sum_{i=1}^{i=12} Tavg_i}{12}$	°C
Bio-2 diurnal temperature range	$Bio2 = \frac{\sum_{i=1}^{i=12} (Tmax_i - Tmin_i)}{12}$	°C
Bio-3 isothermality	$Bio3 = \frac{Bio2}{Bio7} \times 100$	%
Bio-4 temperature variation in a year	$Bio4 = SD\{Tavg_1, \ldots, Tavg_{12}\} \times 100$	%
Bio-7 annual temperature range	$Bio7 = Bio5 - Bio6$	°C
Seasonal temperature indicators		
Bio-5 maximum monthly temperature	$Bio5 = \max(\{Tmax_1, \ldots, Tmax_{12}\})$	°C
Bio-6 minimum monthly temperature	$Bio6 = \min(\{Tmin_1, \ldots, Tmin_{12}\})$	°C
Bio-10 mean temperature of the warmest quarter	$Q_{max} = max\begin{pmatrix} \sum_{i=1}^{i=3} Tavg_i \\ \sum_{i=2}^{i=4} Tavg_i \\ \ldots, \\ \sum_{i=11}^{i=1} Tavg_i \\ \sum_{i=12}^{i=2} Tavg_i \end{pmatrix}$	
	$Bio10 = \frac{\sum_{i=1}^{i=3} Tavg_i}{3}$, based on the three selected months of Q_{max}	°C
Bio-11 mean temperature of the coldest quarter	$Q_{min} = min\begin{pmatrix} \sum_{i=1}^{i=3} Tavg_i \\ \sum_{i=2}^{i=4} Tavg_i \\ \ldots, \\ \sum_{i=11}^{i=1} Tavg_i \\ \sum_{i=12}^{i=2} Tavg_i \end{pmatrix}$	
	$Bio11 = \frac{\sum_{i=1}^{i=3} Tavg_i}{3}$, based on the three selected months of Q_{min}	°C
Limiting environment indicators		
Bio-8 mean temperature of the wettest quarter	$Q_{max} = max\begin{pmatrix} \sum_{i=1}^{i=3} Rainfall_i \\ \sum_{i=2}^{i=4} Rainfall_i \\ \ldots, \\ \sum_{i=11}^{i=1} Rainfall_i \\ \sum_{i=12}^{i=2} Rainfall_i \end{pmatrix}$	
	$Bio8 = \frac{\sum_{i=1}^{i=3} Tavg_i}{3}$, based on the three selected months of Q_{max}	°C
Bio-9 mean temperature of the driest quarter	$Q_{min} = min\begin{pmatrix} \sum_{i=1}^{i=3} Rainfall_i \\ \sum_{i=2}^{i=4} Rainfall_i \\ \ldots, \\ \sum_{i=11}^{i=1} Rainfall_i \\ \sum_{i=12}^{i=2} Rainfall_i \end{pmatrix}$	
	$Bio9 = \frac{\sum_{i=1}^{i=3} Tavg_i}{3}$, based on the three selected months of Q_{min}	°C

In Bio-8 and Bio-9 (Bio-10 and Bio-11) equations, the rainfall (temperature) are evaluated for consecutive 3 months, which may span over two consecutive years

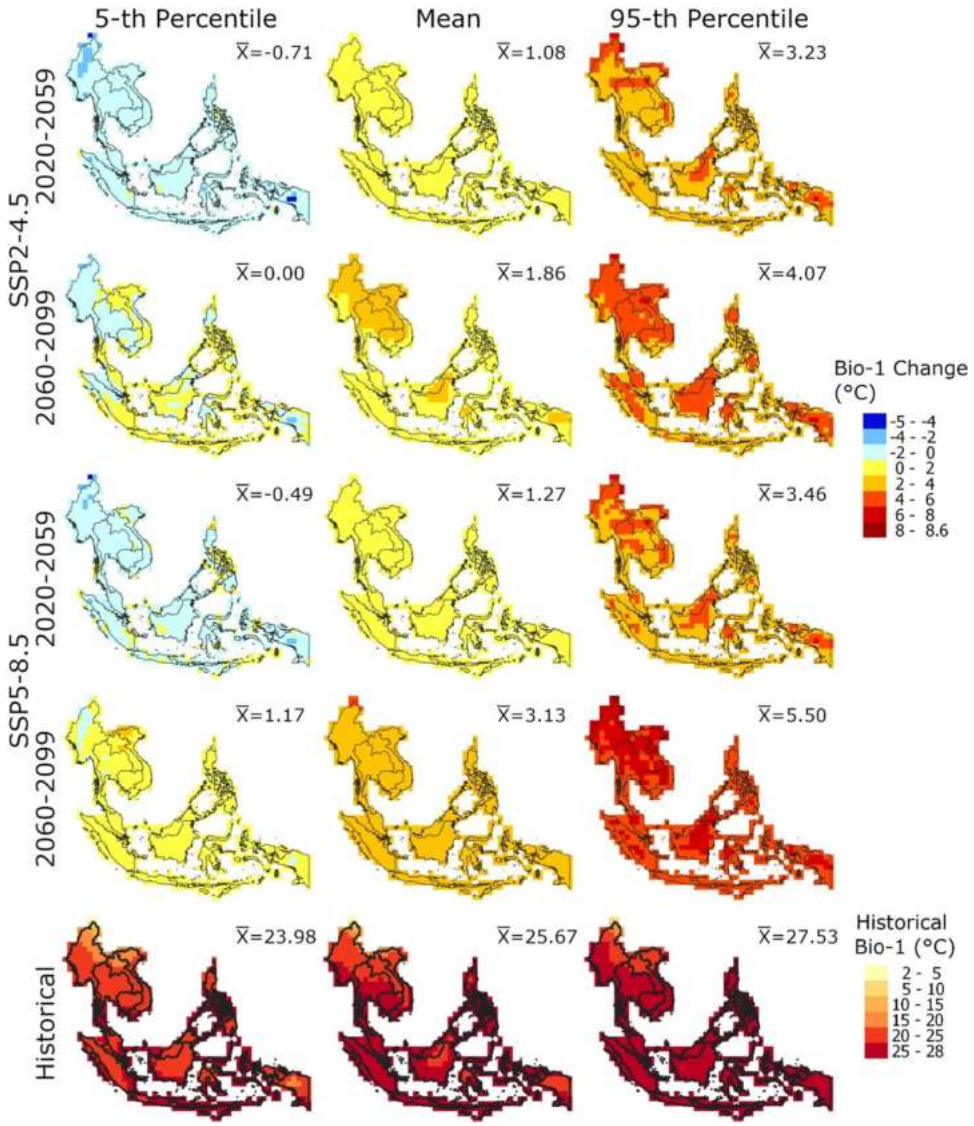

Fig. 2 Spatial distribution of changes in annual mean temperature (Bio-1) for SSP2-4.5 and SSP5-8.5 in near and far futures along with their historical values

temperature range (DTR) or Bio-2 is presented in Fig. 3. Topography had a remarkable impact on the spatial distribution of Bio-1 and Bio-2 across SEA. Bio-1 was low in the northern and southern mountains and high in the plains, while Bio-2 was the opposite. The DTR in SEA is generally low due to its nearness to the equator. A higher increase in T_{min} than T_{max} implies a drop in Bio-2 in many locations of the world resulting from global warming (Karoly et al. 2003; Shahid et al. 2012). It can be observed that the historical MME Bio-1 was the opposite of Bio-2.

The MME mean (with 5th to 95th percentiles) of projected Bio-1 revealed an increase of 1.08 °C (−0.71 to 3.23 °C) and 1.86 °C (0.0 to 4.07 °C) for near and far futures for SSP2-4.5 over the SEA. The increase in mainland SEA would be nearly 2.89 °C above historical levels. The projected MME mean and CI in Bio-1 are almost the for SSP5-8.5 and SSP2-4.5 in the near future. However, the increase in the far future would be by 3.13 °C (1.17 to 5.50 °C), indicating more uncertainty in the projection in the far future and SSP5-8.5 than near future and SSP2-4.5. On the other hand, the MME projected a change in mean with CI in Bio-2 by 0.03 °C (−2.5 to 3.15 °C) and −0.03 °C (−2.50 to 3.00 °C) for SSP2-4.5, and 0.00 °C (−2.48 to 3.09 °C) and −0.05 °C (−2.50 to 2.94 °C) for SSP5-8.5, for the near and far futures. In addition, there are no major variations in areal means of 5th and 95th percentiles for different scenarios.

Isothermality, seasonality, and range

The spatial distribution of historical isothermality (Bio-3) and its future projection over SEA are shown in Fig. 4. Bio-3

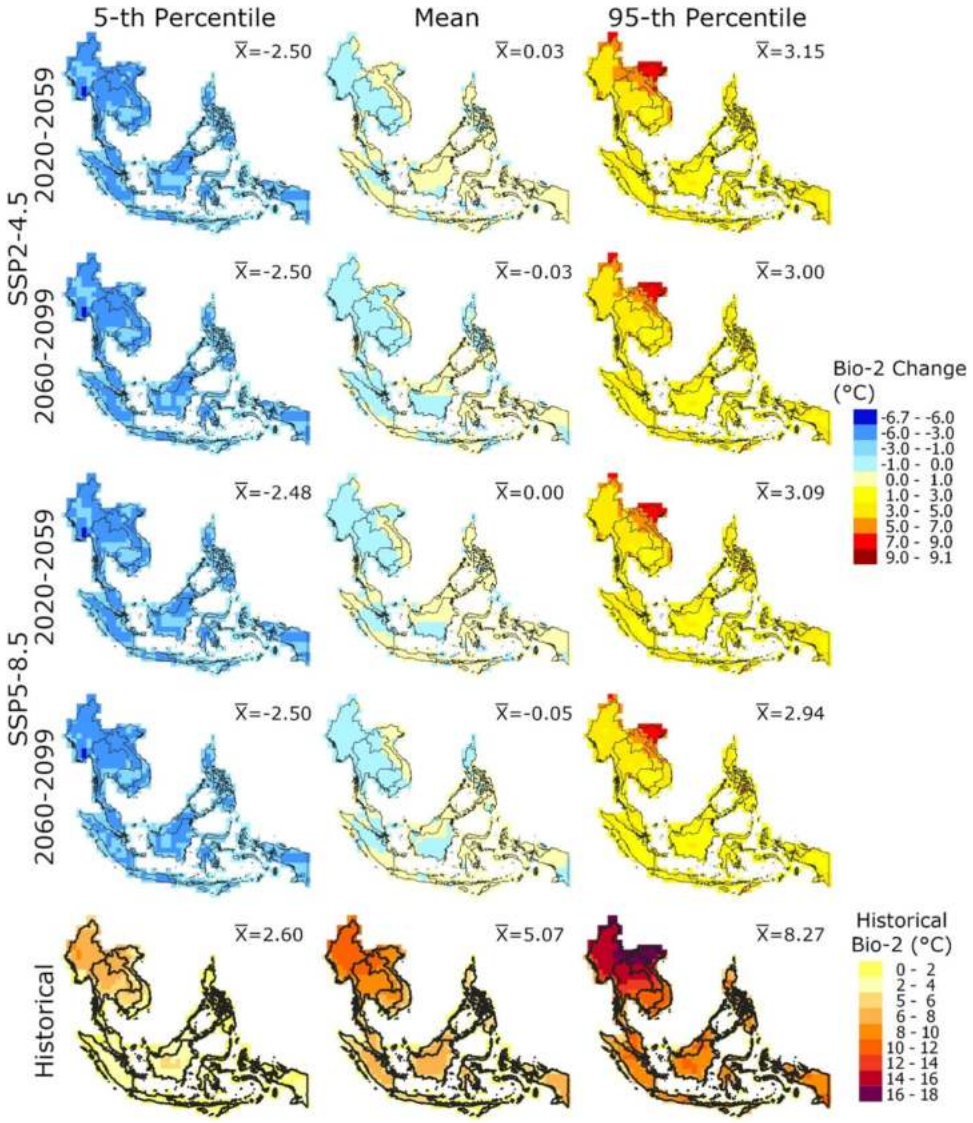

Fig. 3 Spatial distribution of changes in diurnal temperature range (Bio-2) for SSP2-4.5 and SSP5-8.5 in near and far futures along with their historical values

is the ratio of the annual mean diurnal temperature range (Bio-2) to the annual temperature range (Bio-7). A Bio-3 < 100% indicates smaller diurnal temperature variability as compared to annual variability. The GCMs estimated higher values of Bio-3 over the maritime SEA and less in the mainland SEA, as shown in Figs. 4 and 5. For SSP2-4.5, MME showed a change ranging from −3.4 to 0.7% during the near future and −4.6 to 1.4% during the far future. The CI in the change ranges −14.9−13.25% and −15.3−12.5% in the near and far future, respectively. The lowest increase would be in the southern coastal region and the highest in the central region of SEA (i.e., the Philippines). For SSP5-8.5, MME mean (CI) changes are expected to be −0.5% (−15.0 to 13.04%) and −1.28% (−16.0 to 12.2%) for the near and far futures, respectively. The locations with high Bio-3 in the historical period, like Indonesia and Sarawak in Malaysia, show unremarkable change for the different future scenarios.

The seasonality of temperature (Bio-4) is the amount of temperature fluctuation averaged over the years, estimated based on standard deviation in percentage (O'Donnell and Ignizio, 2012). An increase in Bio-4 indicates a greater temperature fluctuation (variability) (Hijmans 2004; O'Donnell and Ignizio 2012). The spatial distribution of Bio-4 indicates a non-homogeneous variability pattern over SEA, which is opposite of the distribution of annual mean temperature. The mean Bio-4 is less over the south SEA (Indonesia, Malaysia, Brunei, and Singapore) and high in the north. The projected changes in the MME mean and CI of Bio-4 showed more or less similar spatial distribution for different scenarios. The MME change in Bio-4 is about 1.36% (−4.10 to 2.90%) for SSP2-4.5, and 0.68% (−4.06 to 5.03%) for SSP5-8.5, for the near future, while 0.38% (−4.21 to 6.31%) for SSP2-4.5 and −0.51% (−2.52 to 2.63%) for SSP5-8.5 for the far future.

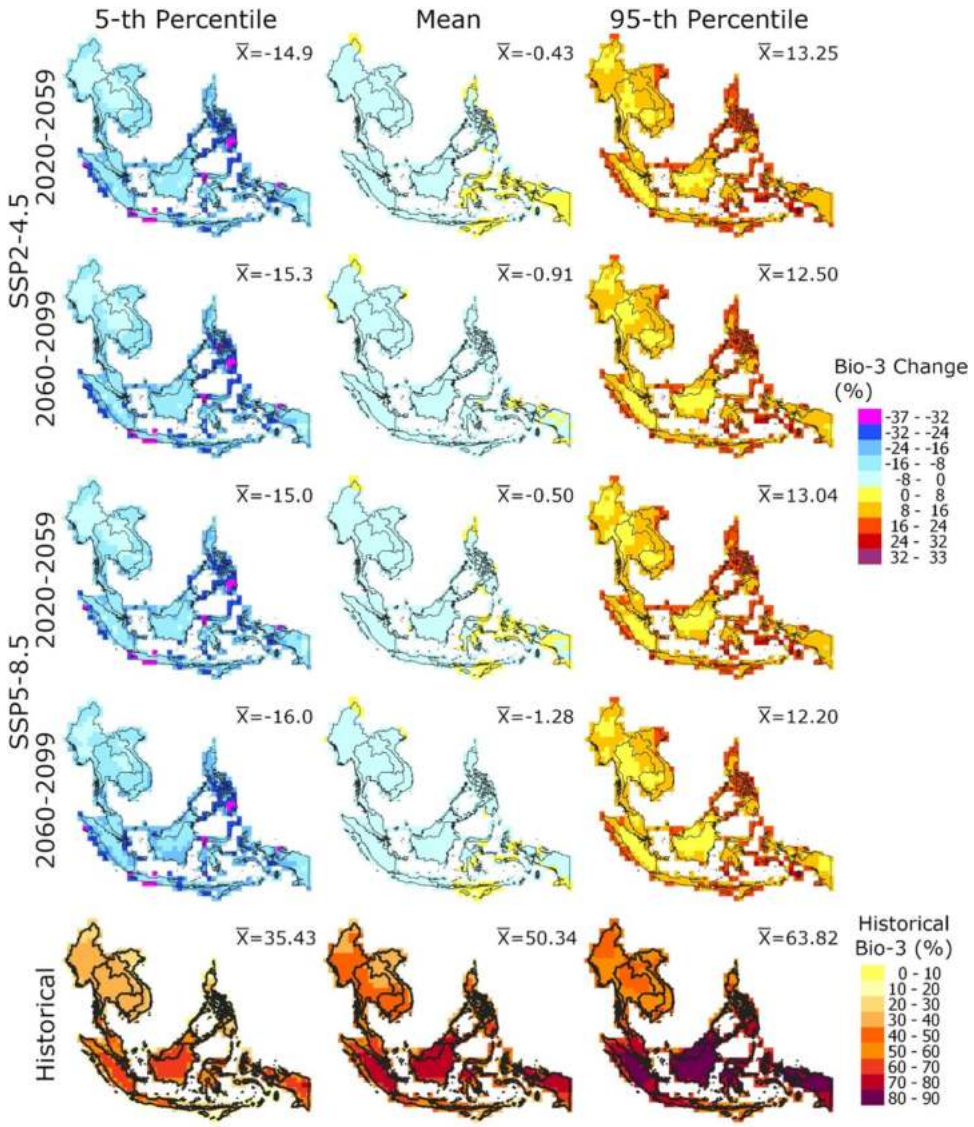

Fig. 4 Spatial distribution of changes in temperature isothermally (Bio-3) for SSP2-4.5 and SSP5-8.5 in near and far futures along with their historical values

Figure 6 presents the annual temperature range (Bio-7) for the historical period and its possible changes in future scenarios in the SEA region. Bio-7 is the temperature variation during a certain period or the difference between Bio-5 and Bio-6. The highest historical value of Bio-7 was in the north region (Myanmar, Thailand, Laos, and Vietnam), and the lowest was in the southeast (North Maluku). The Bio-7 is projected to change by 0.11 °C (− 3.66 to 4.10 °C) and 0.10 °C (− 3.68 to 4.05 °C) in the near and far futures, respectively for SSP2-4.5, while 0.08 °C (− 3.58 to 4.06 °C) and 0.13 °C (− 3.64 to 4.00 °C) in the near and far futures, respectively for SSP5-8.5. The lowest and the largest change would be in the mainland SEA. The main change for each scenario and each future period would be more in the north (mainland SEA).

Seasonal indicators

Mean maximum and minimum monthly temperature

The maximum monthly temperature (Bio-5) and minimum monthly temperature (Bio-6) during the historical period over SEA, along with two future scenarios (SSP2-4.5 and 5–8.5), are presented in Figs. 7 and 8, respectively. The highest historical values of Bio-5 are observed in Thailand and southern Myanmar and the lowest in northern Myanmar. The lowest Bio-6 values are noticed in northern Myanmar and the highest in the coastal regions of Indonesia, Brunei, and the Philippines.

The Bio-5 is projected to change by 1.17 °C (− 2.03 to 4.63 °C) and 1.98 °C (− 1.40 to 5.48 °C) for the near and far futures for SSP2-4.5, while 1.35 °C (− 1.79 to 4.90 °C)

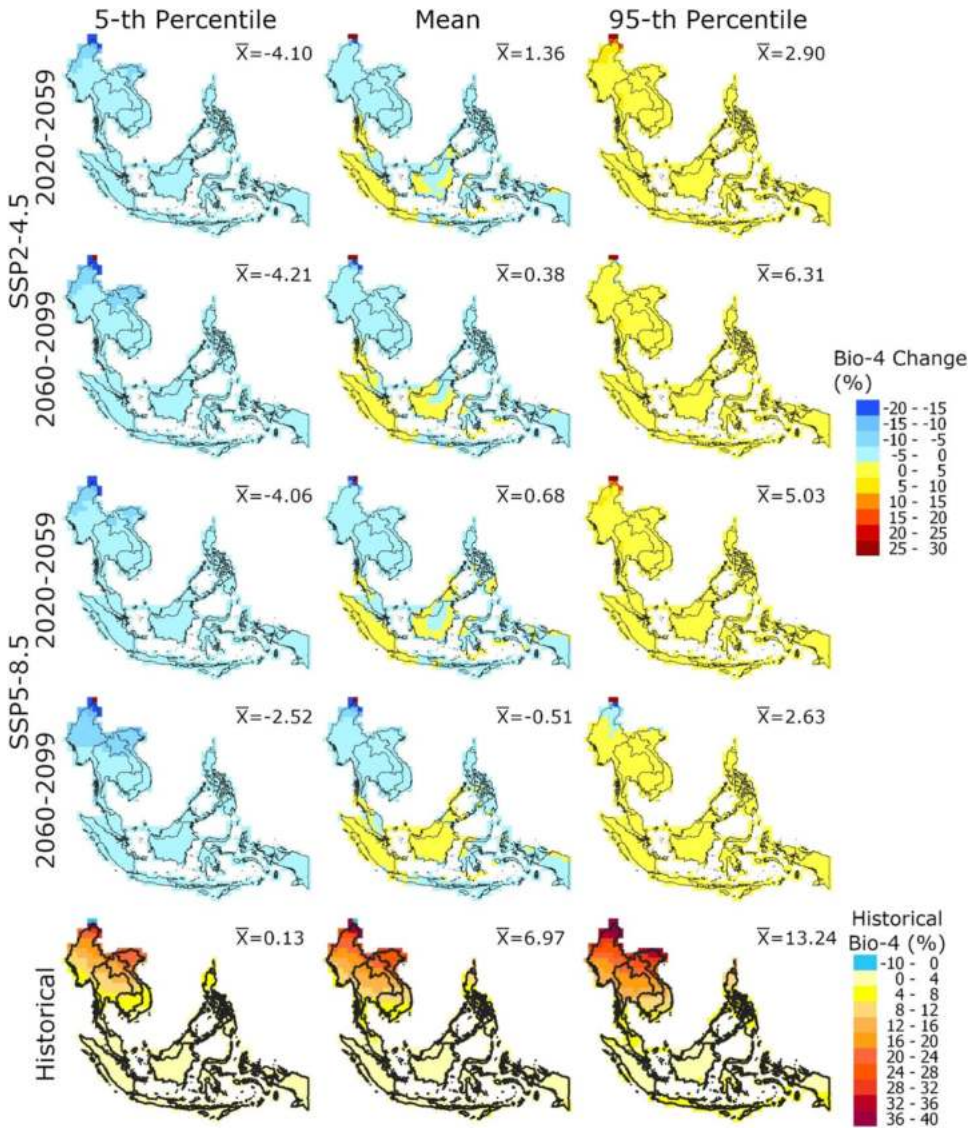

Fig. 5 Spatial distribution of changes in temperature seasonality (Bio-4) for SSP2-4.5 and SSP5-8.5 in near and far futures along with their historical values

and 3.27 °C (− 0.29 to 7.07 °C) for the near and far futures for SSP5-8.5. However, the changes in Bio-6 are projected 1.06 °C (− 1.39 to 3.50 °C) and 1.88 °C (− 0.60 to 4.31 °C) for SSP2-4.5 and 1.27 °C (− 1.20 to 3.71 °C) and 3.15 °C (0.69 to 5.69 °C) for SSP5-8.5, for the near and far futures, respectively. It indicates a higher increase in Bio-6 than Bio-5 in SEA. For both indicators, the highest future change would be in the far future for SSP5-8.5, especially in the north of Myanmar.

Mean temperature of the warmest and coldest quarters

The mean temperature for the consecutive 3 months at each grid point was computed to determine the warmest and coldest quarters. Like the selection of maximum and minimum temperature months, a dynamic method was used to select the warmest and coldest quarters. The mean temperature of the warmest quarter (Bio-10) and mean temperature of the coldest quarter (Bio-11) during the historical period over SEA, along with two future scenarios (SSP2-4.5 and 5–8.5), are presented in Figs. 9 and 10, respectively. Both indicators have the same historical spatial distribution over SEA. The lowest values of these indicators occur in the north and the highest in the Indonesian coastal regions. Both indicators follow the geography of SEA, where the mountain regions show the lower values and plain lands show higher values. The mean changes in Bio-11 were similar to that for Bio-10, for both futures and SSPs.

For SSP2-4.5, the CI of the projected changes in Bio-10 was − 0.93−3.60 °C for the near future, while − 0.2−4.50 °C for the far future. On the other hand, the changes in CI of Bio-11 are − 0.84−3.28 °C for the near future and − 0.05−4.07 °C for the far future. There

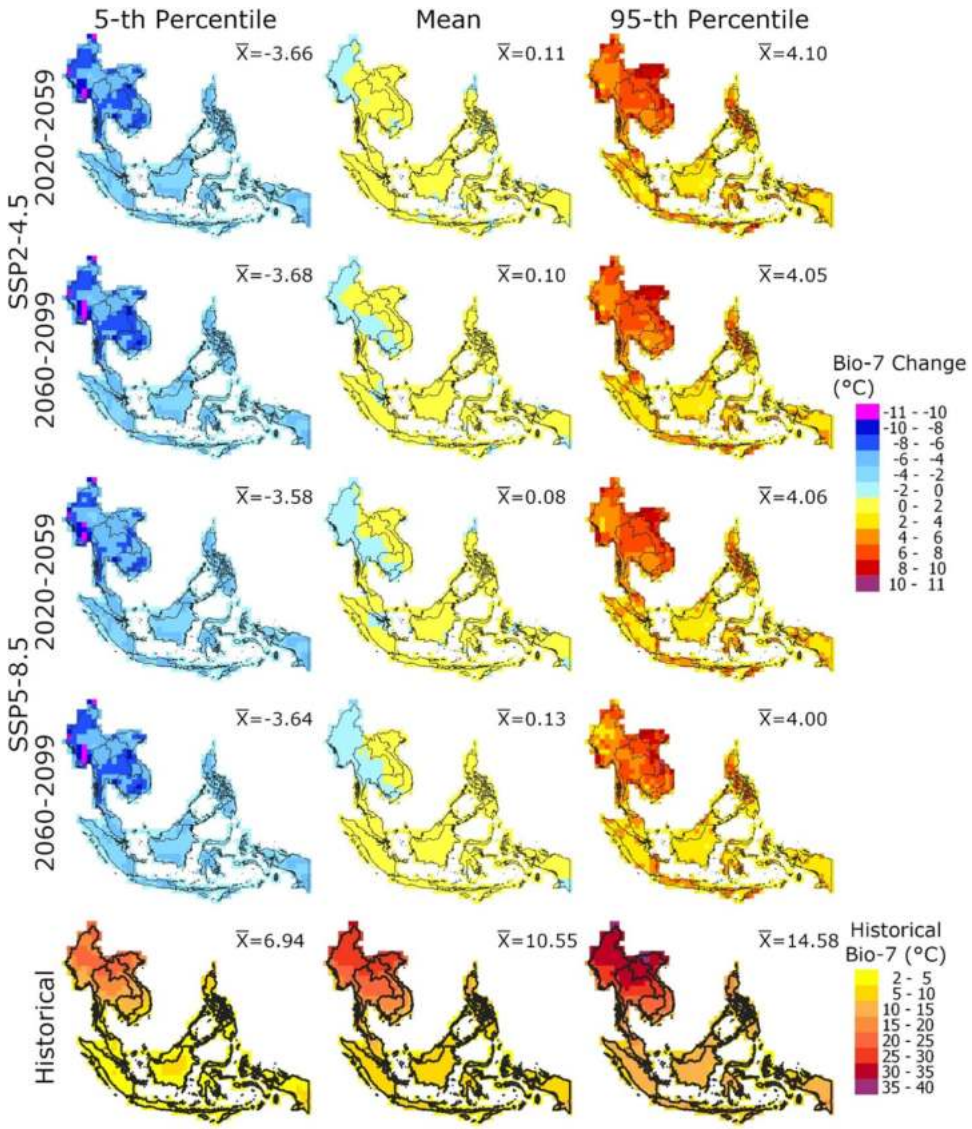

Fig. 6 Spatial distribution of changes in annual temperature range (Bio-7) for SSP2-4.5 and SSP5-8.5 in near and far futures along with their historical values

are no differences in the near future projections between SSP5-8.5 and SSP2-4.5 for both indicators. However, in the far future, the CI of the projected changes are 0.87−6.04 °C for Bio-10 and 1.16−5.45 °C for Bio-11, respectively. The greatest changes were projected in the north for all scenarios and future periods. It is observed that the increase in mean temperature of the coldest quarter is higher than the warmest quarter in all scenarios and future periods.

Limiting environment indicators

The SEA has a varied climate, and therefore, rainfall distribution varies considerably throughout the year. The rainfall for the three successive months was computed for each grid point to select the wettest and driest quarters. The mean temperature of the wettest quarter (Bio-8) and mean temperature of the driest quarter (Bio-9) during the historical period over SEA, along with two future scenarios (SSP2-4.5 and 5–8.5), are presented in Figs. 11 and 12, respectively. Both indicators have the same distribution pattern in the historical period. The lowest values are in the north of Myanmar, and the highest values are in the southern coastal regions.

The projected change in the mean and CI of Bio-8 are expected to be 1.04 °C (− 0.75 to 3.10 °C) for the near and 1.76 °C (− 0.03 to 3.89 °C) for the far futures for SSP2-4.5. Those are for Bio-9 were 1.12 °C (− 0.94 to 3.68 °C) in the near and 1.95 °C (− 0.16 to 4.50 °C) in the far future. For SSP5-8.5, the changes in Bio-8 are expected to 1.21 °C (− 0.55 to 3.32 °C) in the near and 2.97 °C (− 1.11 to 5.33 °C) in the far future, while 1.33 °C (− 0.72 to 3.87 °C) in the near and 3.22 °C (1.00 to 5.97 °C) in the far future for Bio-9. North Myanmar showed the highest uncertainty

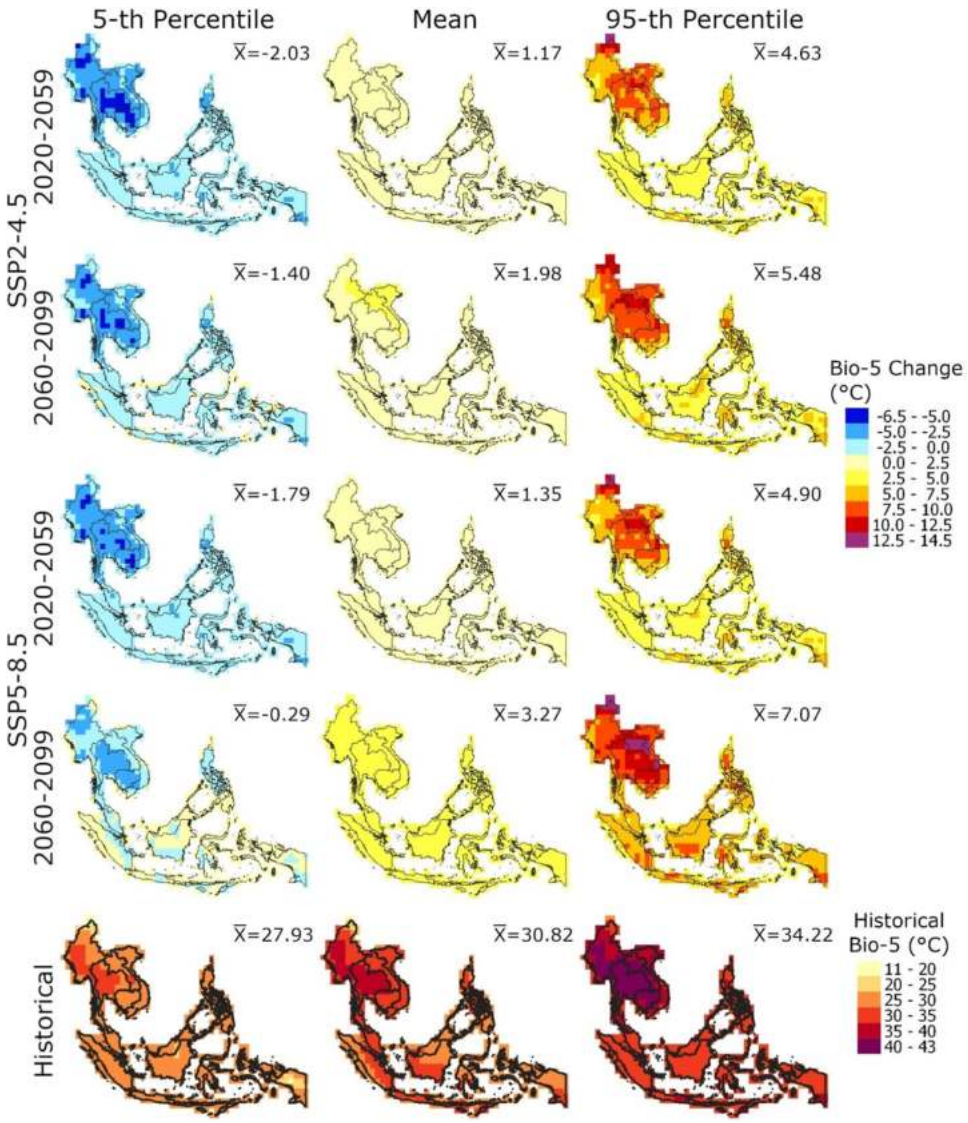

Fig. 7 Spatial distribution of changes in diurnal maximum temperature in the warmest month (Bio-5) for SSP2-4.5 and SSP5-8.5 in near and far futures along with their historical values

in projections of these indicators for all SSPs and future periods. Both indicators showed similar spatial distribution in the changes.

Discussion

The present study assessed the existing spatial distribution of eleven thermal bioclimatic indicators in SEA and their projections for two SSPs. These eleven indicators are used to provide information on different thermal conditions meaningfully related to the biology and ecology of SEA. The study revealed that the mean temperature (Bio-1) in SEA would increase between 1.08 and 1.86 °C for SSP2-4.5, which agrees with Supharatid et al. (2022). However, the projected rise in temperature in SEA would be much less than in many other regions (Alamgir et al. 2019; Khan et al. 2020; Shiru et al. 2020; Hamed et al. 2022b). This also agrees with the findings of O'Gorman and Schneider (2009) and Trewin (2014). The spatial distribution of the changes in different bio-climatic indicators (Table 3) showed higher sensitivity of bio-climate to climate change in the north of SEA. All indicators are projected to increase in the north except DTR and isothermality. The increase in the annual temperature range indicates that hot extremes will continue to increase in the north. Despite an increase in minimum temperature, the cold extreme may not diminish considerably. The spatial distribution of Bio-4 indicates an increase in the east and north of SEA, while a decrease in the central and southwest regions, which is opposite to the annual mean temperature distribution. It means that temperature would become more variable in the region where it is low and more stable in the region where it is high. It means the

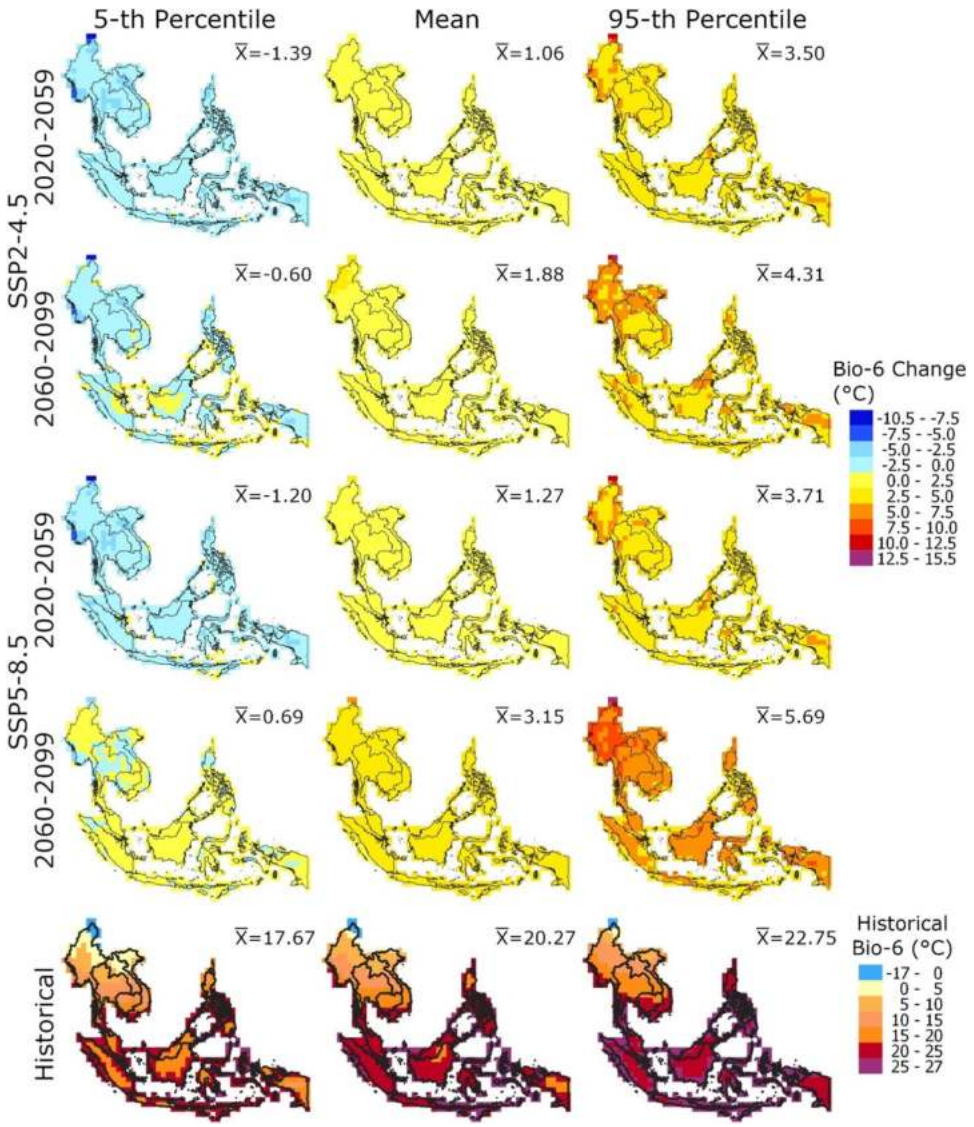

Fig. 8 Spatial distribution of changes in minimum temperature in the coldest month (Bio-6) for SSP2-4.5 and SSP5-8.5 in near and far futures along with their historical values

temperature variability would gradually decrease in the higher temperature region, which would make the region less prone to temperature extremes. The opposite would be noticed in the lower temperature region in the east and north.

The temperature isothermally (Bio-3) is projected to decrease by − 4 to − 16% in most SEA. The decrease will be higher in the east of SEA, which has a dense species distribution. The decrease in Bio-2 and Bio-3 would remarkable impact the niche of many species and public health (Ehbrecht et al. 2019). The effect of climate change on temperature seasonality was small (− 5 to 5%) for all scenarios. This would be due to an increase in both the annual temperature range and DTR. The relative increase of both indicators would keep the temperature seasonality constant throughout the century. The temperature in both the warmest and coldest months would increase in SEA. However, the increase would be more in the coldest month than in the warmest month. In contrast, the temperature increase in the warmest and coldest quarters would be more or less the same. The increase in the wettest quarter would be more than the driest quarter. This indicates a possible increase in both humidity and temperature in the wettest months, which may negatively affect human comfort. The increased temperature in the driest quarter might increase water stress and forest fire.

Two methods are generally employed to consider the shifts in the warmest/coldest month or quarter. They can be reselected for the future period or can be kept fixed based on the historical period (Bede-Fazekas and Somodi 2020). The dynamic method guarantees the selection of the warmest/coldest month or quarter for both historical and future periods. However, it ignores the possible shift in seasonal temperature variability. In contrast, fixing the

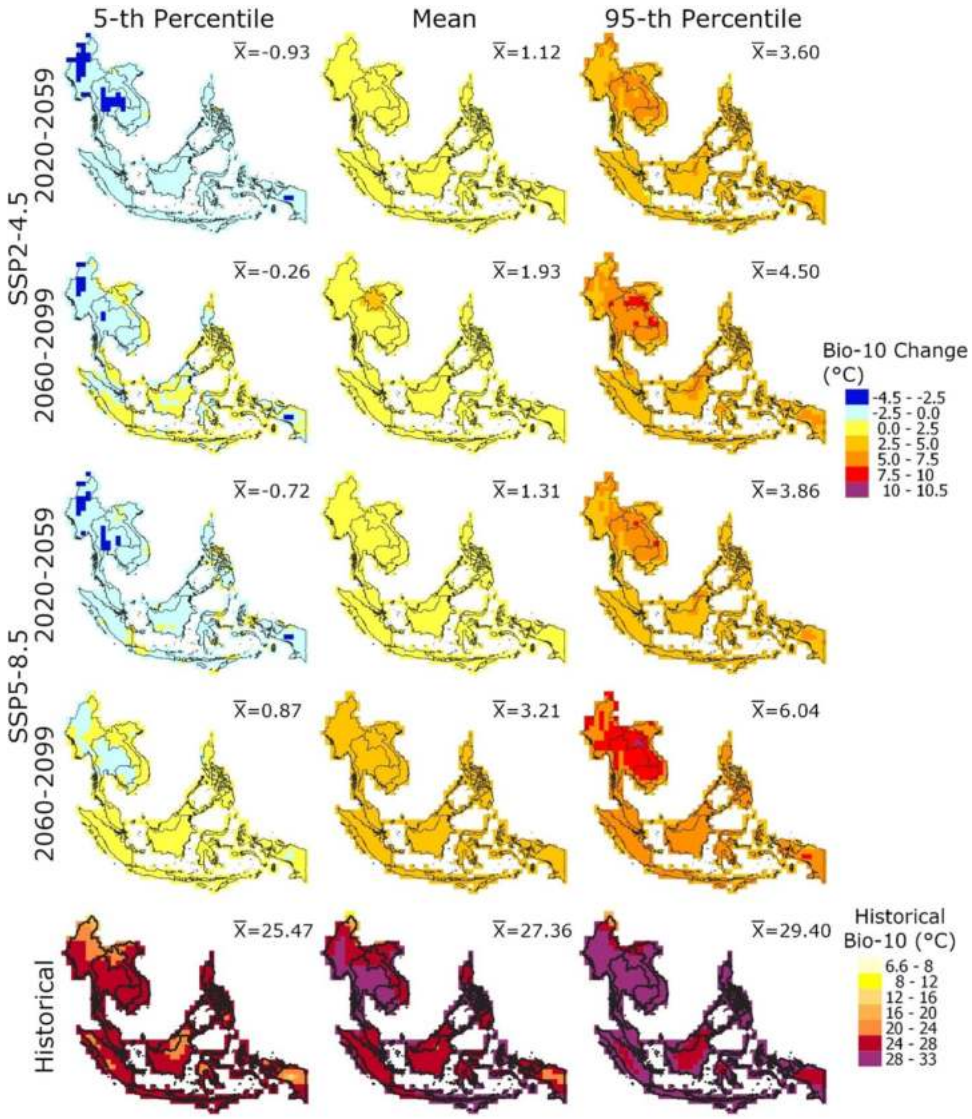

Fig. 9 Spatial distribution of changes in mean temperature of the warmest quarter (Bio-10) for SSP2-4.5 and SSP5-8.5 in near and far futures along with their historical values

warmest/coldest month or quarter based on a historical period may breach the definition of the indicator for future periods. Bede-Fazekas and Somodi (2020) evaluated the relative performance of the two methods and suggested not to consider one superior to another. The present study adopted the second approach. It ignored possible climate shifts in the future. Therefore, the presented results of Bio-5 to Bio-11 should be interpreted with caution. In the future, studies can be conducted to assess the shifts in the warmest/coldest month/quarter for different SSPs and future periods to provide better insight and selection of the most appropriate method of calculating the changes in these indicators.

Identifying the climatic drivers of the geographical distribution of plants and animals, particularly the factors prompting changes in their spatial range over time, is vital for ecologists, biogeographers, and conservation biologists (Braby et al. 2014). Changes in global climate have affected ecology and the environment in many across the globe (Bede-Fazekas and Somodi 2020). Several studies reported the projected effect of climate change on different species in SEA using CMIP5 (Kolanowska and Konowalik 2014; Bernardes 2016; Tan et al. 2017; Setyawan et al. 2018). Tan et al. (2017) results showed severe implications, such as disruption, habitat loss, extinction, and migration of species in SEA. Setyawan et al. (2018) used 4 RCPs models from CMIP5 for the potential niche distribution of selaginellas. The dataset and maps of the spatial distribution of bioclimatic indicators generated in this study would help determine the niche distribution for the present climate. Besides, the maps can be used to identify the occurrence location of different species.

Previous studies related to the projection of bioclimatic indicators are based on CMIP5 models and RCP scenarios

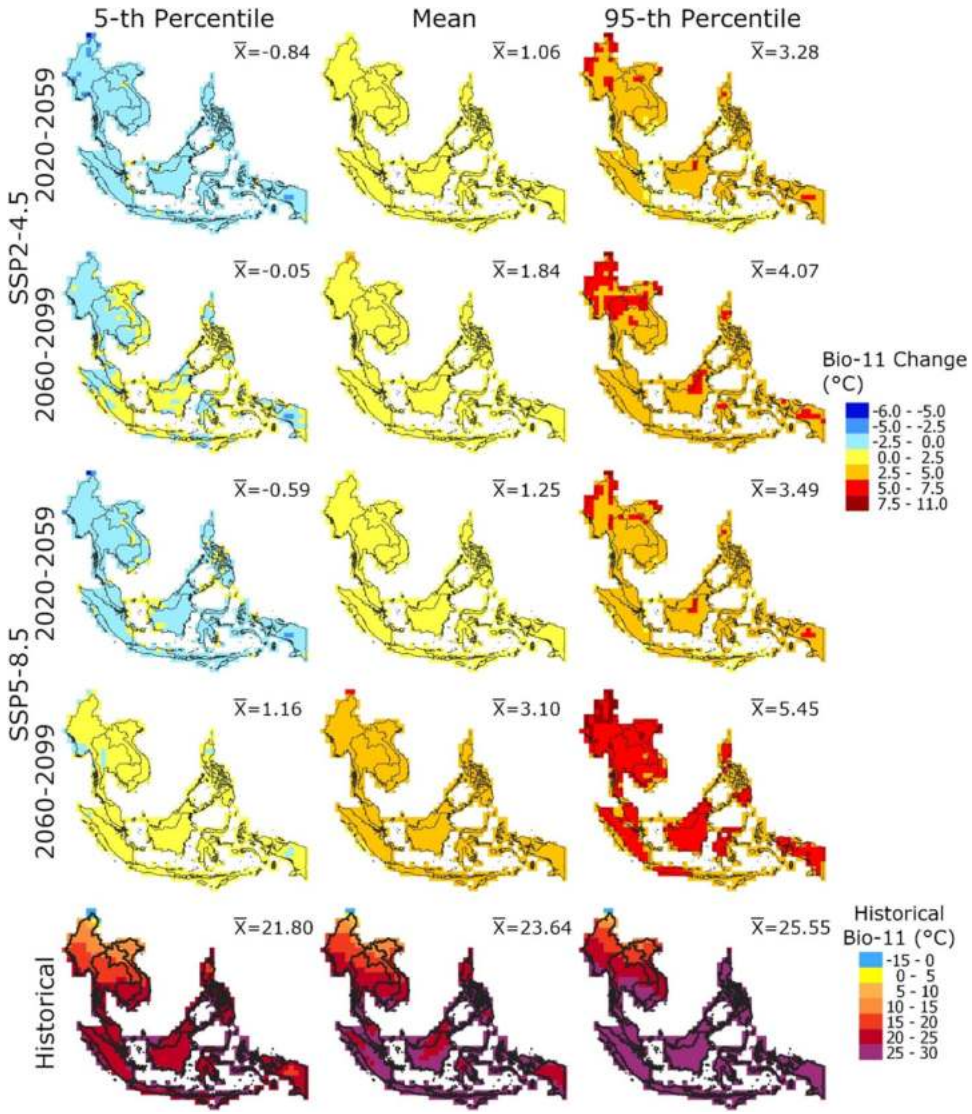

Fig. 10 Spatial distribution of changes in mean temperature of coldest quarter (Bio-11) for SSP2-4.5 and SSP5-8.5 in near and far futures along with their historical values

(Phillips and Bonfils 2015; Navarro-Racines et al. 2019; Noce et al. 2020). Noce et al. (2020) calculated different global bioclimatic indicators at 0.5° by 0.5° resolution for historical periods and RCP4.5 and RCP8.5 scenarios. They disseminated projected data through an open portal but did not show the projections of global bioclimate. However, analysis of their data showed an increase in temperature in SEA, but less than the global average as found in our study. The CMIP6 GCMs have some advantages, including enhancement in model structure, spatial resolution, uncertainty, and representing synoptic progressions (Eyring et al. 2016; Song et al. 2021; Su et al. 2021; Hamed et al. 2022a, b). Therefore, it is vital to reassess the effects for new scenarios using CMIP6 to update the knowledge of climate change implications on species distribution and rationalize the adaptation strategies planned based on CMIP5 projections.

Uncertainties associated with GCMs hinder the reliable projection of extreme temperature (Pour et al. 2018; Shiru et al. 2019, 2020). Generally, projection uncertainties are minimized using GCMs ensemble, selected according to their ability to replicate the observed climate (Lutz et al. 2016; Salman et al. 2019, 2020; Khan et al. 2020; Nashwan and Shahid 2020; Hamed et al. 2022c). The present study estimated the spatial distribution of the changes in thermal bioclimatic indicators at a 90% confidence interval. The uncertainty in the changes can provide better insight into the possible wide range of changes in the bio-environment of SEA.

The SEA has experienced a rapid change in land use in recent decades. The areal coverage of tropical forests has been reduced unremarkably in the last five decades. The restoration of forests for carbon sequestration and as a clean development mechanism has been given priority in different

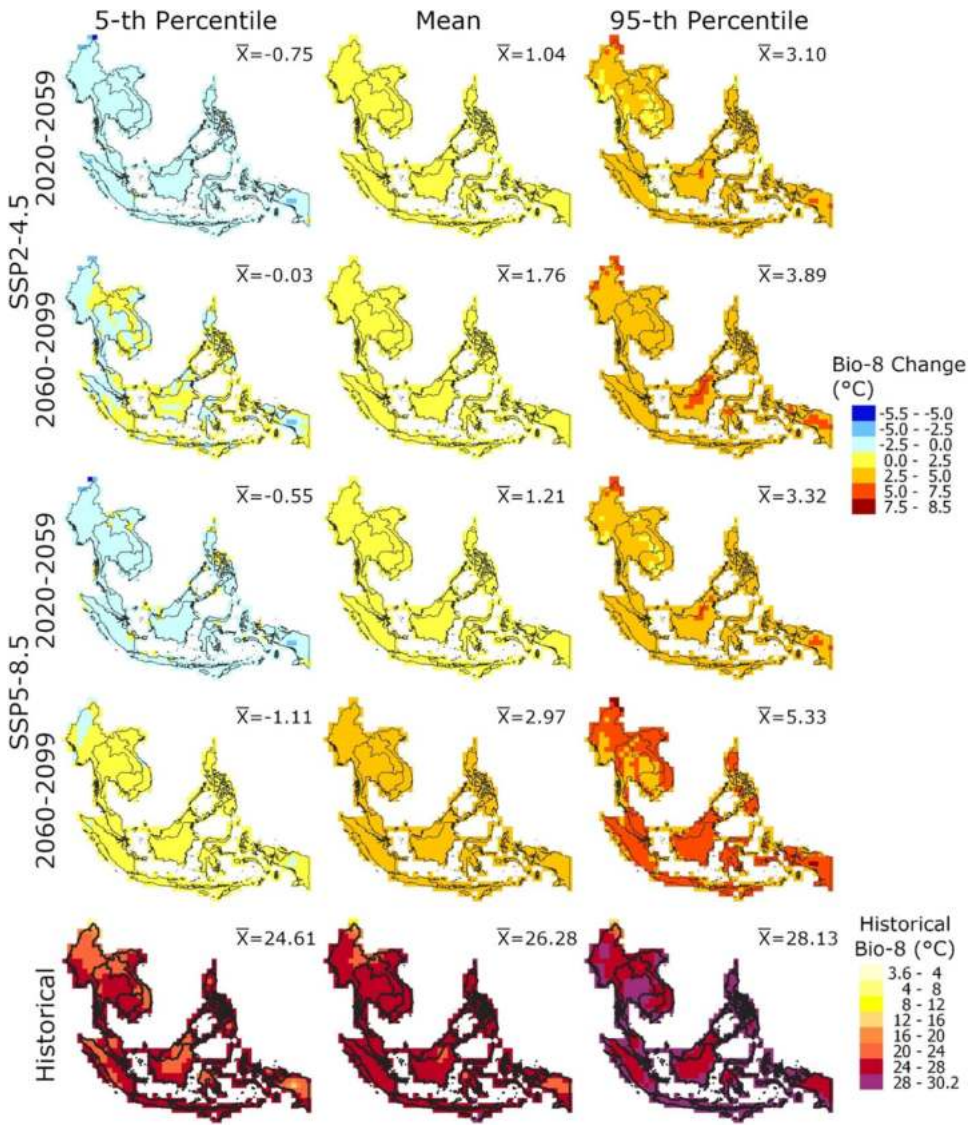

Fig. 11 Spatial distribution of changes in mean temperature of the wettest quarter (Bio-8) for SSP2-4.5 and SSP5-8.5 in near and far futures along with their historical values

SEA countries to combat global warming. The spatial distribution of bioclimatic indicators and their projections can play a strong role in this regard (Booth 2004). It can be used to assess which species could be promoted for which region. For example, Pangahas, (2003) used bioclimatic indicators to demarcate the suitable lands for forest refurbishment in the Philippines.

Mitigating climate change impacts on building energy consumption is a major challenge. Wong et al. (2012) showed an increase in heat stress in SEA, and thus, a possible increase in energy use and higher carbon emissions. Thermal bioclimatic indicators can reliably provide an estimation of building energy use. Therefore, projected changes in thermal bioclimatic indicators can be used to assess the changes in future building energy consumption in SEA for different SSPs. Bioclimatic indicators can also be used to evaluate the performance of energy-efficient buildings under climate change scenarios to identify the suitable building design for different regions of SEA.

Thermal bioclimatic indicators are also directly linked to disease spread and public health. Several studies showed that high temperatures favored larval development leading to faster disease vector population growth. Studies also revealed that temperature is positively related to disease vector activity. The geographical distribution of the projections of thermal bioclimatic indicators can be used to evaluate the changes in the favorable condition of vector-borne diseases, and thus, their possible spread in different regions. It can also be used to assess how the newly emerged disease can spread over SEA. For example, Gao et al. (2020) used bioclimatic indicators to predict the high-risk zones of possible transmission of a sub-Saharan virus if spread over SEA.

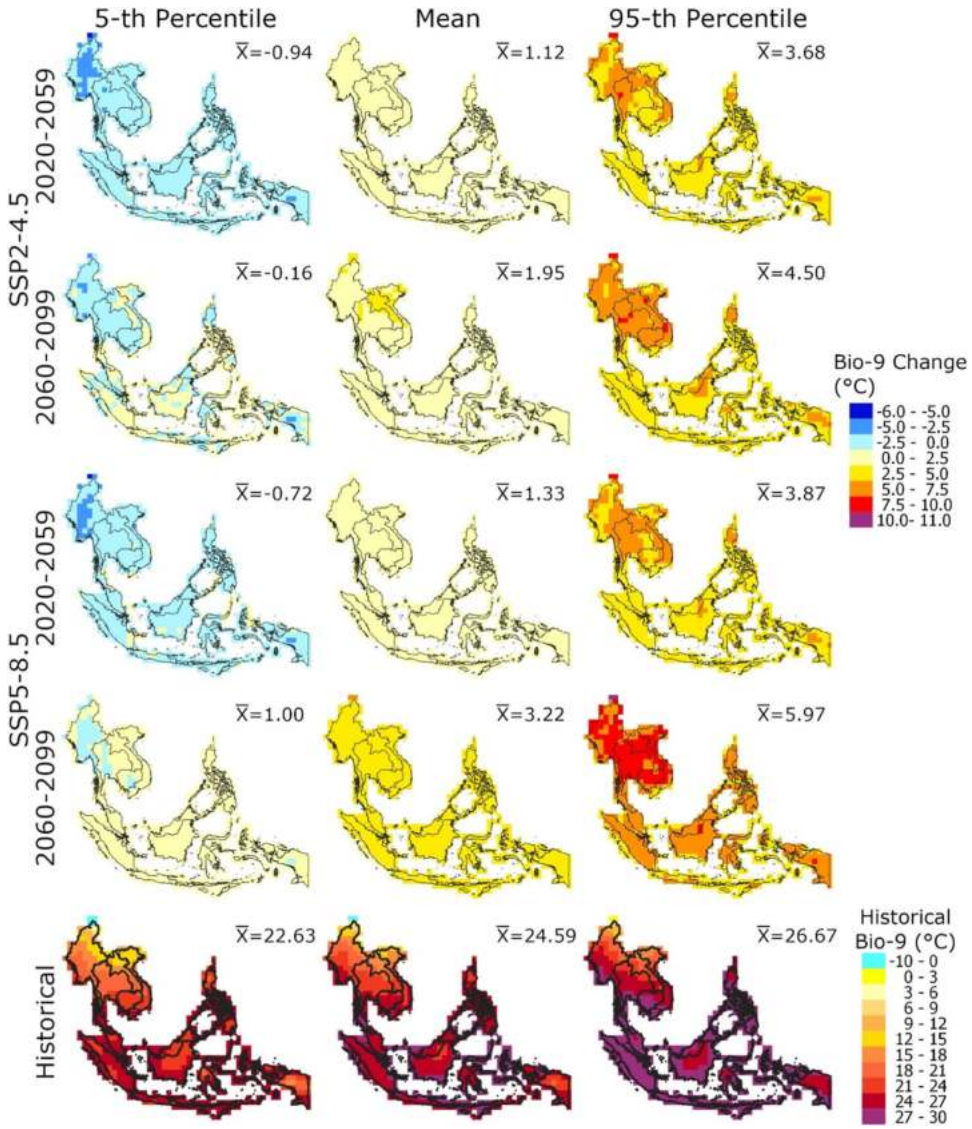

Fig. 12 Spatial distribution of changes in mean temperature of the driest quarter (Bio-9) for SSP2-4.5 and SSP5-8.5 in near and far futures along with their historical values

Table 3 Summary of the spatial distribution of the changes in thermal bio-indicators

Indicator	Changes	
	Increase	Decrease
Annual indicators		
Bio-1 annual mean temperature	All over SEA. The higher increase in the north	-
Bio-2 diurnal temperature range	East, south, and central	West and north
Bio-3 isothermality	Central and west	East
Bio-4 temperature variation in a year	East, north, and northeast	Central and southwest
Bio-7 annual temperature range	North	All over SEA, except in the north
Seasonal temperature indicators		
Bio-5 maximum monthly temperature	All over SEA. The higher increase in the north	-
Bio-6 minimum monthly temperature	All over SEA. The higher increase in the north	-
Bio-10 mean temperature of the warmest quarter	All over SEA. The higher increase in the north	-
Bio-11 mean temperature of the coldest quarter	All over SEA. The higher increase in the north	-
Limiting environment indicators		
Bio-8 mean temperature of the wettest quarter	All over SEA, mostly at the same rate	-
Bio-9 mean temperature of the driest quarter	All over SEA. The higher increase in the north	-

Conclusions

The present study assessed the geographical distribution of only 11 thermal bioclimatic indicators in SEA and their possible spatiotemporal variability in the future with associated uncertainties. The future projections were limited to only medium and high (SSP2-4.5 and 5–8.5) emission scenarios. The mean MME and 90% confidence interval of the projections of 23 GCMs were used. The study revealed an increase in mean and seasonal temperatures over the entire SEA. However, the temperature would rise more in the warmest or wettest quarters compared to cold or dry quarters. This could cause an increase in the annual temperature range. A decrease in diurnal temperature range and increase in annual temperature range may lead to a decrease in their ratio and, thus, isothermality. A decrease in seasonality at the same time may cause a shift in the climate pattern in some parts of SEA. Environmental and conservation scientists can use maps and information generated in this study to understand possible changes or shifts in biodiversity with regard to climate change. It can also be used by the governments of SEA for sustainable development planning. Future studies can be conducted to evaluate changes in other bioclimatic indicators related to rainfall and humidity. Other SSPs, such as SSP1-1.9, 1–2.6 and 3–7.0, can also be used in the future. Besides, species' sensitivity to the projected climate can be estimated to assess risk and potential migration over space.

Author contribution All authors contributed to the conception and design of the study. MMH, MSN, and SS collected data and analyzed them. All authors contributed to writing the first draft. TI, AD, and MA repeatedly edited the paper to prepare the final version of the manuscript.

Funding The authors are grateful to Staffordshire University, UK, for providing financial support for this research through grant no. WR GCRF 2020–2021.

Data availability All datasets of the thermal bioclimatic indicators (Historical, SSP2-4.5 and SSP5-8.5) are available at Figshare (https://doi.org/10.6084/m9.figshare.19310939.v1). The dataset consists of 11 historical thermal bioclimatic (*.tif) files and their projections for SSP2-4.5 and SSP5-8.5 in the near and far futures.

Declarations

Ethics approval The manuscript has not been submitted to more than one journal for simultaneous consideration. No data, text, or theories by others are presented in our manuscript.

Consent to participate The authors do not have any person's data in any form.

Competing interests The authors declare no competing interests.

References

Abdullah MT (2003) Biogeography and variation of Cynopterus brachyotis in Southeast Asia. University of Queensland. Available https://espace.library.uq.edu.au/view/UQ:106221

Abe M, Kitoh A, Yasunari T (2003) An evolution of the Asian summer monsoon associated with mountain uplift - simulation with the MRI atmosphere-ocean coupled GCM. J Meteorol Soc Japan 81:909–933. https://doi.org/10.2151/jmsj.81.909

Alamgir M, Ahmed K, Homsi R et al (2019) Downscaling and projection of spatiotemporal changes in temperature of Bangladesh. Earth Syst Environ 3:381–398. https://doi.org/10.1007/s41748-019-00121-0

Asadollah SBHS, Khan N, Sharafati A, et al (2021) Prediction of heat waves using meteorological variables in diverse regions of Iran with advanced machine learning models. Stoch Environ Res Risk Assess 0123456789https://doi.org/10.1007/s00477-021-02103-z

Asif F (2019) From sea to city: migration and social well-being in coastal Cambodia BT - urban climate resilience in Southeast Asia. In: Daniere AG, Garschagen M (eds) The Urban Book Series. Springer International Publishing, Cham, pp 149–177

Banerjee AK, Mukherjee A, Guo W et al (2019) Combining ecological niche modeling with genetic lineage information to predict potential distribution of Mikania micrantha Kunth in South and Southeast Asia under predicted climate change. Glob Ecol Conserv 20:e00800

Bede-Fazekas Á, Somodi I (2020) The way bioclimatic variables are calculated has impact on potential distribution models. Methods Ecol Evol 11:1559–1570. https://doi.org/10.1111/2041-210X.13488

Bellard C, Bertelsmeier C, Leadley P et al (2012) Impacts of climate change on the future of biodiversity. Ecol Lett 15:365–377. https://doi.org/10.1111/j.1461-0248.2011.01736.x

Bernardes S (2016) Predicted responses of vegetation to climate change: a global analysis of changes in primary productivity and water use efficiency in the 21st century. In: AGU Fall Meeting Abstracts. pp B33E–0674. Available https://ui.adsabs.harvard.edu/abs/2016AGUFM.B33E0674B

Booth TH (2004) Using bioclimatic analysis to assist tropical reforestation for biodiversity and carbon sequestration benefits. Kyoto Mech Conserv Trop For Ecosyst 163–171

Boucher O, Denvil S, Levavasseur G, et al (2018) IPSL IPSL-CM6A-LR model output prepared for CMIP6 CMIP

Braby MF, Bertelsmeier C, Sanderson C, Thistleton BM (2014) Spatial distribution and range expansion of the Tawny Coster butterfly, Acraea terpsicore (Linnaeus, 1758) (Lepidoptera: Nymphalidae), in South-East Asia and Australia. Insect Conserv Divers 7:132–143. https://doi.org/10.1111/icad.12038

Çaliskan O, Türkoglu N, Matzarakis A (2013) The effects of elevation on thermal bioclimatic conditions in Uludağ (Turkey). Atmósfera 26:45–57

Cao J, Wang B (2019) NUIST NESMv3 model output prepared for CMIP6 CMIP. https://doi.org/10.22033/ESGF/CMIP6.2021

Chai Z (2020) CAS CAS-ESM2.0 model output prepared for CMIP6 CMIP. https://doi.org/10.22033/ESGF/CMIP6.1944

Daham A, Han D, Matt Jolly W et al (2018) Predicting vegetation phenology in response to climate change using bioclimatic indices in Iraq. J Water Clim Chang 10:835–851. https://doi.org/10.2166/wcc.2018.142

Dai Y, Peng G, Wen C et al (2021) Climate and land use changes shift the distribution and dispersal of two umbrella species in the Hindu Kush Himalayan region. Sci Total Environ 777:146207. https://doi.org/10.1016/j.scitotenv.2021.146207

Dix M, Bi D, Dobrohotoff P et al (2019) CSIRO-ARCCSS ACCESS-CM2 model output prepared for CMIP6 CMIP historical. https://doi.org/10.22033/ESGF/CMIP6.4271

Döscher R, Acosta M, Alessandri A et al (2021) The EC-Earth3 Earth System Model for the Climate Model Intercomparison Project 6. Geosci Model Dev Discuss 2021:1–90. https://doi.org/10.5194/gmd-2020-446

Duanmu L, Sun X, Jin Q, Zhai Z (2017) Relationship between human thermal comfort and indoor thermal environment parameters in various climatic regions of China. Procedia Eng 205:2871–2878. https://doi.org/10.1016/j.proeng.2017.09.913

Eckstein D, Künzel V, Schäfer L (2017) Global climate risk index 2018. Ger Bonn. Available http://cambioclimaticohn.org/uploaded/content/article/303643999.pdf

Ehbrecht M, Schall P, Ammer C et al (2019) Effects of structural heterogeneity on the diurnal temperature range in temperate forest ecosystems. For Ecol Manage 432:860–867. https://doi.org/10.1016/j.foreco.2018.10.008

Eyring V, Bony S, Meehl GA et al (2016) Overview of the Coupled Model Intercomparison Project Phase 6 (CMIP6) experimental design and organization. Geosci Model Dev 9:1937–1958. https://doi.org/10.5194/gmd-9-1937-2016

Gao H, Bie J, Wang H et al (2020) Modelling high-risk areas for african horse sickness occurrence in mainland China along Southeast Asia. Authorea 1–11. https://doi.org/10.22541/au.160570106.63915759/v1

Ge F, Zhu S, Peng T et al (2019) Risks of precipitation extremes over Southeast Asia: does 1.5 °C or 2 °C global warming make a difference? Environ Res Lett 14:044015. https://doi.org/10.1088/1748-9326/aaff7e

Hamed MM, Nashwan MS, Shahid S (2021) Performance evaluation of reanalysis precipitation products in Egypt using fuzzy entropy time series similarity analysis. Int J Climatol 41:5431–5446. https://doi.org/10.1002/joc.7286

Hamed MM, Nashwan MS, Shahid S et al (2022a) Inconsistency in historical simulations and future projections of temperature and rainfall: a comparison of CMIP5 and CMIP6 models over Southeast Asia. Atmos Res 265:105927. https://doi.org/10.1016/j.atmosres.2021.105927

Hamed MM, Nashwan MS, Shahid S (2022b) Inter-comparison of historical simulation and future projection of rainfall and temperature by CMIP5 and CMIP6 GCMs over Egypt. Int J Climatol n/a:1–17. https://doi.org/10.1002/joc.7468

Hamed MM, Nashwan MS, Shahid S (2022c) A novel selection method of CMIP6 GCMs for robust climate projection. Int J Climatol 42:4258–4272. https://doi.org/10.1002/joc.7461

Hijmans RJ (2004) Arc Macro Language (AML®) version 2.1 for calculating 19 bioclimatic predictors: Berkeley, Calif, Museum of Vertebrate Zoology. Univ Calif Berkeley Available http://www.worldclim.org/bioclim. Accessed 1 Mar 2022

Hu X-G, Jin Y, Wang X-R et al (2015) Predicting impacts of future climate change on the distribution of the widespread conifer Platycladus orientalis. PLoS One 10:e0132326

Huang W (2019) THU CIESM model output prepared for CMIP6 CMIP historical. https://doi.org/10.22033/ESGF/CMIP6.8843

IPCC (2007) Climate change 2007-the physical science basis: working group I contribution to the fourth assessment report of the IPCC. Available http://www.amazon.com/Climate-Change-2007-Contribution-Assessment/dp/0521880092

Iqbal Z, Shahid S, Ahmed K et al (2021) Evaluation of CMIP6 GCM rainfall in mainland Southeast Asia. Atmos Res 254:105525. https://doi.org/10.1016/j.atmosres.2021.105525

Karoly DJ, Karl B, Stott PA et al (2003) Detection of a human influence on North American climate. Science 302(80-):1200–1203. https://doi.org/10.1126/science.1089159

Khadka D, Babel MS, Abatan AA, Collins M (2021) An evaluation of CMIP5 and CMIP6 climate models in simulating summer rainfall in the Southeast Asian monsoon domain. Int J Climatol n/ahttps://doi.org/10.1002/joc.7296

Khan N, Shahid S, Ahmed K et al (2020) Selection of GCMs for the projection of spatial distribution of heat waves in Pakistan. Atmos Res 233:104688. https://doi.org/10.1016/j.atmosres.2019.104688

Kolanowska M, Konowalik K (2014) Niche conservatism and future changes in the potential area coverage of Arundina graminifolia, an invasive orchid species from Southeast Asia. Biotropica 46:157–165. https://doi.org/10.1111/btp.12089

Krasting JP, John JG, Blanton C, et al (2018) NOAA-GFDL GFDL-ESM4 model output prepared for CMIP6 CMIP. Earth Syst Grid Fed Version 20220101. https://doi.org/10.22033/ESGF/CMIP6.1407

Kriticos DJ, Webber BL, Leriche A et al (2012) CliMond: global high-resolution historical and future scenario climate surfaces for bioclimatic modelling. Methods Ecol Evol 3:53–64. https://doi.org/10.1111/j.2041-210X.2011.00134.x

Kuo C-C, Gan TY, Wang J (2020) Climate change impact to Mackenzie river Basin projected by a regional climate model. Clim Dyn 54:3561–3581. https://doi.org/10.1007/s00382-020-05177-7

Lau N-C, Nath MJ (2000) Impact of ENSO on the variability of the Asian-Australian monsoons as simulated in GCM experiments. J Clim 13:4287–4309. https://doi.org/10.1175/1520-0442(2000)013%3c4287:IOEOTV%3e2.0.CO;2

Lutz AF, ter Maat HW, Biemans H et al (2016) Selecting representative climate models for climate change impact studies: an advanced envelope-based selection approach. Int J Climatol 36:3988–4005. https://doi.org/10.1002/joc.4608

Mochizuki T, Igarashi H, Sugiura N et al (2007) Improved coupled GCM climatologies for summer monsoon onset studies over Southeast Asia. Geophys Res Lett 34:1–7. https://doi.org/10.1029/2006GL027861

Molloy SW, Davis RA, Van Etten EJB (2014) Species distribution modelling using bioclimatic variables to determine the impacts of a changing climate on the western ringtail possum (Pseudocheirus occidentals; Pseudocheiridae). Environ Conserv 41:176–186. https://doi.org/10.1017/S0376892913000337

Moron V, Navarra A, Ward MN, Roeckner E (1998) Skill and reproducibility of seasonal rainfall patterns in the tropics in ECHAM-4 GCM simulations with prescribed SST. Clim Dyn 14:83–100. https://doi.org/10.1007/s003820050211

Nashwan MS, Ismail T, Ahmed K (2018) Flood susceptibility assessment in Kelantan river basin using copula. Int J Eng Technol 7:584–590. https://doi.org/10.14419/ijet.v7i2.8876

Nashwan MS, Shahid S (2020) A novel framework for selecting general circulation models based on the spatial patterns of climate. Int J Climatol 40:4422–4443. https://doi.org/10.1002/joc.6465

Nasional BPP (2012) National Action Plan for Climate Change Adaptation (RAN-API)

Navarro-Racines CE, Tarapues Montenegro JE, Thornton PK et al (2019) CCAFS-CMIP5 Delta Method Downscaling for monthly averages and bioclimatic indices of four RCPs. World Data Cent Clim DKRZ. Available https://cera-www.dkrz.de/WDCC/ui/cerasearch/entry?acronym=CCAFS-CMIP5_downscaling

Noce S, Caporaso L, Santini M (2020) A new global dataset of bioclimatic indicators. Sci Data 1–12https://doi.org/10.1038/s41597-020-00726-5

O'Donnell MS, Ignizio DA (2012) Bioclimatic predictors for supporting ecological applications in the conterminous United States. US Geol Surv Data Ser 691:10

O'Gorman PA, Schneider T (2009) The physical basis for increases in precipitation extremes in simulations of 21st-century climate change. Proc Natl Acad Sci 106:14773–14777. https://doi.org/10.1073/pnas.0907610106

Pangahas NN (2003) Ecological restoration of the Philippine dipterocarp forest ecosystems: the role of spatial, meso-scale climatic modelling. The Australian National University. https://doi.org/10.25911/5d51583839f68

Peano D, Lovato T, Materia S (2020) CMCC CMCC-ESM2 model output prepared for CMIP6 LS3MIP. https://doi.org/10.22033/ESGF/CMIP6.13165

Peel MC, Finlayson BL, McMahon TA (2007) Updated world map of the Köppen-Geiger climate classification. Hydrol Earth Syst Sci 11:1633–1644. https://doi.org/10.1002/ppp.421

Phillips TJ, Bonfils CJW (2015) Köppen bioclimatic evaluation of CMIP historical climate simulations. Environ Res Lett 10https://doi.org/10.1088/1748-9326/10/6/064005

Pour SH, Shahid S, Chung ES, Wang XJ (2018) Model output statistics downscaling using support vector machine for the projection of spatial and temporal changes in rainfall of Bangladesh. Atmos Res 213:149–162. https://doi.org/10.1016/j.atmosres.2018.06.006

Pour SH, Wahab AKA, Shahid S, Wang X (2019) Spatial pattern of the unidirectional trends in thermal bioclimatic indicators in Iran. Sustain 11https://doi.org/10.3390/su11082287

Pu Y, Liu H, Yan R et al (2020) CAS FGOALS-g3 model datasets for the CMIP6 Scenario Model Intercomparison Project (ScenarioMIP). Adv Atmos Sci 37:1081–1092. https://doi.org/10.1007/s00376-020-2032-0

Ragheb AA, El-Darwish II, Ahmed S (2016) Microclimate and human comfort considerations in planning a historic urban quarter. Int J Sustain Built Environ 5:156–167. https://doi.org/10.1016/j.ijsbe.2016.03.003

Raitzer D, Bosello F, Tavoni M et al (2015) Southeast Asia and the economics of global climate stabilization. Asian Dev Bank

Redfern SK, Azzu N, Binamira JS (2012) Rice in Southeast Asia: facing risks and vulnerabilities to respond to climate change. Build Resil Adapt Clim Chang Agri Sect 23:1–14

Rehfeldt GE, Worrall JJ, Marchetti SB, Crookston NL (2015) Adapting forest management to climate change using bioclimate models with topographic drivers. For an Int J for Res 88:528–539. https://doi.org/10.1093/forestry/cpv019

Ribeiro MM, Roque N, Ribeiro S et al (2019) Bioclimatic modeling in the Last Glacial Maximum, mid-Holocene and facing future climatic changes in the strawberry tree (Arbutus unedo L.). PLoS One 14:e0210062

Robertson AW, Moron V, Qian J et al (2011) The maritime continent monsoon. In: the global monsoon system. World Sci 5:85–98. https://doi.org/10.1142/9789814343411_0006

Salehie O, Hamed MM, Ismail T, bin, Shahid S, (2022a) Projection of droughts in Amu river basin for shared socioeconomic pathways CMIP6. Theor Appl Climatol. https://doi.org/10.1007/s00704-022-04097-2

Salehie O, Ismail T, Hamed MM et al (2022b) Projection of hot and cold extremes in the Amu river basin of Central Asia using GCMs CMIP6. Stoch Environ Res Risk Assess. https://doi.org/10.1007/s00477-022-02201-6

Salehie O, Ismail TB, Shahid S et al (2022c) Assessment of water resources availability in Amu Darya river basin using GRACE data. Water 14:533. https://doi.org/10.3390/w14040533

Salman SA, Nashwan MS, Ismail T, Shahid S (2020) Selection of CMIP5 general circulation model outputs of precipitation for peninsular Malaysia. Hydrol Res 51:781–798. https://doi.org/10.2166/nh.2020.154

Salman SA, Shahid S, Ismail T et al (2019) Selection of gridded precipitation data for Iraq using compromise programming. Meas J Int Meas Confed 132:87–98. https://doi.org/10.1016/j.measurement.2018.09.047

Schiemann R, Demory M-E, Mizielinski MS et al (2014) The sensitivity of the tropical circulation and maritime continent precipitation to climate model resolution. Clim Dyn 42:2455–2468. https://doi.org/10.1007/s00382-013-1997-0

Semmler T, Danilov S, Rackow T et al (2018) AWI AWI-CM1.1MR model output prepared for CMIP6 CMIP 1pctCO2. https://doi.org/10.22033/ESGF/CMIP6.2543

Setyawan AD, Supriatna J, Nisyawati N et al (2018) Predicting impacts of future climate change on the distribution of the widespread selaginellas (Selaginella ciliaris and S. plana) in Southeast Asia. Biodiversitas 19:1960–1977. https://doi.org/10.13057/biodiv/d190548

Shahid S, Bin HS, Katimon A (2012) Changes in diurnal temperature range in Bangladesh during the time period 1961–2008. Atmos Res 118:260–270. https://doi.org/10.1016/j.atmosres.2012.07.008

Shiru MS, Chung ES, Shahid S, Alias N (2020) GCM selection and temperature projection of Nigeria under different RCPs of the CMIP5 GCMS. Theor Appl Climatol 141:1611–1627. https://doi.org/10.1007/s00704-020-03274-5

Shiru MS, Shahid S, Chung E-SS et al (2019) A MCDM-based framework for selection of general circulation models and projection of spatio-temporal rainfall changes: a case study of Nigeria. Atmos Res 225:1–16. https://doi.org/10.1016/j.atmosres.2019.03.033

Sintayehu DW (2018) Impact of climate change on biodiversity and associated key ecosystem services in Africa: a systematic review. Ecosyst Heal Sustain 4:225–239. https://doi.org/10.1080/20964129.2018.1530054

Song YH, Nashwan MS, Chung ES, Shahid S (2021) Advances in CMIP6 INM-CM5 over CMIP5 INM-CM4 for precipitation simulation in South Korea. Atmos Res 247:105261. https://doi.org/10.1016/j.atmosres.2020.105261

Song Z, Qiao F, Bao Y et al (2019) FIO-QLNM FIO-ESM2.0 model output prepared for CMIP6 CMIP historical. https://doi.org/10.22033/ESGF/CMIP6.9199

Su B, Huang J, Mondal SK et al (2021) Insight from CMIP6 SSP-RCP scenarios for future drought characteristics in China. Atmos Res 250:105375. https://doi.org/10.1016/j.atmosres.2020.105375

Supharatid S, Nafung J (2021) Projected drought conditions by CMIP6 multimodel ensemble over Southeast Asia. J Water Clim Chang 12:3330–3354. https://doi.org/10.2166/wcc.2021.308

Supharatid S, Nafung J, Aribarg T (2022) Projected changes in temperature and precipitation over mainland Southeast Asia by CMIP6 models. J Water Clim Chang 13:337–356. https://doi.org/10.2166/wcc.2021.015

Swart NC, Cole JNS, Kharin VV et al (2019) The Canadian Earth System Model version 5 (CanESM5.0.3). Geosci Model Dev 12:4823–4873. https://doi.org/10.5194/gmd-12-4823-2019

Tan MK, Ingrisch S, Wahab RBHA (2017) First Velarifictorus (Orthoptera: Gryllidae, Gryllinae) cricket described from Borneo (Southeast Asia) and notes on a co-occurring congener. Zootaxa 4282:374–384. https://doi.org/10.11646/zootaxa.4282.2.10

Tatebe H, Ogura T, Nitta T et al (2019) Description and basic evaluation of simulated mean state, internal variability, and climate sensitivity in MIROC6. Geosci Model Dev 12:2727–2765. https://doi.org/10.5194/gmd-12-2727-2019

Theusme C, Avendaño-Reyes L, Macías-Cruz U et al (2021) Climate change vulnerability of confined livestock systems predicted using bioclimatic indexes in an arid region of México. Sci Total Environ 751:141779

Trewin B (2014) The climates of the tropics and how they are changing. State Trop 1:39–52

van Zonneveld M, Koskela J, Vinceti B, Jarvis A (2009) Impact of climate change on the distribution of tropical pines in Southeast Asia. Unasylva 60:24–29

Vinke K, Schellnhuber HJ, Coumou D et al (2017) A region at risk: the human dimensions of climate change in Asia and the Pacific. https://doi.org/10.22617/TCS178839-2

Volodin E, Mortikov E, Gritsun A et al (2019a) INM INM-CM4–8 model output prepared for CMIP6 PMIP. https://doi.org/10.22033/ESGF/CMIP6.2295

Volodin E, Mortikov E, Gritsun A et al (2019b) INM INM-CM5–0 model output prepared for CMIP6 CMIP piControl. https://doi.org/10.22033/ESGF/CMIP6.5081

von Storch J-S, Putrasahan D, Lohmann K et al (2017) MPI-M MPIESM1.2-HR model output prepared for CMIP6 HighResMIP. https://doi.org/10.22033/ESGF/CMIP6.762

Waltari E, Schroeder R, McDonald K et al (2014) Bioclimatic variables derived from remote sensing: assessment and application for species distribution modelling. Methods Ecol Evol 5:1033–1042. https://doi.org/10.1111/2041-210X.12264

Wang A, Melton AE, Soltis DE, Soltis PS (2021) Potential distributional shifts in North America of allelopathic invasive plant species under climate change models. Plant Divers. https://doi.org/10.1016/j.pld.2021.06.010

Wieners K-H, Giorgetta M, Jungclaus J et al (2019) MPI-M MPIESM1.2-LR model output prepared for CMIP6 ScenarioMIP ssp245. https://doi.org/10.22033/ESGF/CMIP6.6693

Woetzel J, Pinner D, Samandari H (2020) Climate risk and response. McKinsey Global Institute

Wong SL, Wan KKW, Yang L, Lam JC (2012) Changes in bioclimates in different climates around the world and implications for the built environment. Build Environ 57:214–222. https://doi.org/10.1016/j.buildenv.2012.05.006

Wu T, Chu M, Dong M, et al (2018) BCC BCC-CSM2MR model output prepared for CMIP6 CMIP piControl

Yang S, Wu R, Jian M et al (2021) Climate change in Southeast Asia and surrounding areas. Springer Climate. http://link.springer.com/10.1007/978-981-15-8225-7

Yoon S, Lee W-H (2021) Methodological analysis of bioclimatic variable selection in species distribution modeling with application to agricultural pests (Metcalfa pruinosa and Spodoptera litura). Comput Electron Agric 190:106430. https://doi.org/10.1016/j.compag.2021.106430

Yukimoto S, Kawai H, Koshiro T et al (2019) The Meteorological Research Institute Earth System Model Version 2.0, MRI-ESM2.0: description and basic evaluation of the physical component. J Meteorol Soc Japan Ser II 97:931–965. https://doi.org/10.2151/jmsj.2019-051

Ziehn T, Chamberlain M, Lenton A et al (2019) CSIRO ACCESS-ESM1.5 model output prepared for CMIP6 CMIP. https://doi.org/10.22033/ESGF/CMIP6.2288